Steady states of a column of shaken inelastic beads

B. Bernu
Laboratoire de Physique Théorique des Liquides, Université Pierre et Marie Curie, 4 place Jussieu, 75252 Paris Cedex 05, France

F. Delyon
Centre de Physique Théorique, Ecole Polytechnique, 91128 Palaiseau Cedex, France

R. Mazighi
Laboratoire de Physique Théorique des Liquides, Université Pierre et Marie Curie, 4 place Jussieu, 75252 Paris Cedex 05, France

(Received 18 January 1994; revised manuscript received 27 April 1994)

We study dynamical properties of N inelastic beads shaken by a vibrating plane. These systems exhibit three kinds of steady states, depending on the inelasticity of the beads: a gas, a partially condensed phase, and a collapsed phase. In the one-dimensional case, we show that these phases are characterized by the parameter $\gamma = N(1-\eta)$, where η is the restitution coefficient measuring the energy dissipation during the collisions. For $\gamma < 0.1$ and $1.5 < \gamma < 3.1$, good agreement is found between the one-body distribution function obtained by numerical simulations and analytical solutions.

PACS number(s): 05.20.Dd, 05.40.+j, 05.70.Ln, 46.10.+z

I. INTRODUCTION

Currently, the phenomena associated with granular materials are studied within a variety of scientific and engineering disciplines. For instance, experimental investigations have dealt with avalanches [1–3], segregation phenomenon [4], and instabilities in sandpiles [5,8] submitted to external vibrations, where convection and self-diffusion regimes have been observed [6]. For the description of granular flows [9], various theoretical approaches, based on continuum description [10] as well as kinetic theory [11] or stochastic methods [12], have been done together with computer simulations [13]. Some papers report on two-dimensional granular systems, using experimental techniques [14] or numerical methods where inelastic microstructure also is investigated [15,16]. However, the notion of fluidization [7], in vibrated particulate matter, is still unclarified.

One-dimensional models often facilitate the understanding of specific problems in statistical physics. Here we attempt to describe and quantify the three different phases of vibrated granular media in one dimension, namely, a gas, a partially condensed phase, and a collapsed phase can be observed. By using the same vibration, these three phases appear inside the medium when the damping is increased. We provide analytical solutions of one-body distribution functions and compare them with solutions obtained by numerical simulations.

Consider a column of N beads, in a constant gravitational field g, bouncing on a vibrating plane. For simplicity, all particles have the same mass. At time t, the positions are denoted $z_i(t)$ and the velocities $v_i(t)$. The inelasticity of the collisions is described by the restitution coefficient η ($\eta < 1$) as follows. Two particles i and $i-1$ with incident velocities v_i and v_{i-1} bounce back with velocities v'_i and v'_{i-1}:

$$v'_{i-1} = v_i + \frac{(1-\eta)}{2}(v_{i-1} - v_i),$$
$$v'_i = v_{i-1} - \frac{(1-\eta)}{2}(v_{i-1} - v_i). \tag{1}$$

If particle 1 hits the vibrating plane of infinite mass, its new velocity is $v'_1 = 2V_p - v_1$, where V_p is the plane velocity at the collision time.

The plane has a periodic motion $z_p(t)$ with a period τ_0. The mean square velocity V is defined as

$$V^2 = \frac{1}{\tau_0}\int_0^{\tau_0} V_p^2(t)dt \quad \text{where } V_p(t) = \frac{dz_p(t)}{dt}. \tag{2}$$

Without loss of generality, $z_p(t) = V\tau_0 h(t/\tau_0)$, where $h(t)$ is a periodic function of period 1 which satisfies $\int_0^1 h(t)dt = 0$ and $\int_0^1 \dot{h}^2(t)dt = 1$.

For particles in the bulk, the loss of kinetic energy at each collision is $(\eta^2-1)(v_{i-1}-v_i)^2/4$. However, when the lowest bead collides with the vibrating plane, it bounces back with a larger velocity on average. The plane behaves like an energy source. For a given initial situation, the system reaches a steady state after a transient regime. A permanent energy flow between the vibrating plane and the column remains because the energy provided by the plane is continuously dissipated during the inelastic collisions. These general features (energy dissipation due to the collisions, an energy source supplied by the plane, and a system out of equilibrium) are also relevant in two or three dimensions.

The parameters describing the evolution of the column

$\{N, \eta, g, \tau_0, V\}$ can be reduced to three dimensionless parameters $\{N, \eta, g\tau_0/V\}$. Two-dimensional quantities define the units. Therefore, V and g scale velocities and accelerations, respectively. Time and distance are given in units of V/g and V^2/g.

In the following, the parameters γ (see [18]) and τ

$$\gamma = N(1-\eta), \tag{3}$$

$$\tau = \gamma^{1/2} g\tau_0/V \tag{4}$$

are chosen instead of η and $g\tau_0/V$. For a small number of beads ($N < 10$), various particular behaviors (periodic orbits, bifurcation, and a chaotic transition [17]) can occur. Here only systems with a large number of beads are considered, for which generic behaviors are expected.

In this publication, it is shown that this model can be described by the reduced set of parameters $\{\gamma, \tau\}$, i.e., for fixed γ and large N the behavior does not depend on N. γ measures the effective dissipation in the bulk. Equation (3) allows us to consider the *thermodynamic* limit ($N \to \infty$). Moreover, in real matter η goes to 1 as the radius of the beads decreases. Thus, for a given material, different values of γ can be reached for sufficiently small radius and large N.

An analogous model is studied in [18] in the absence of gravity, with a stationary plane. In that case, the column collapses against the plane at $\gamma = \gamma_c \simeq 3$, while a simple model of independent collision waves provides the main properties of the bounce of the column and gives $\gamma_c = \pi$ for large N. For larger γ, our simulations show that the heap collapses on the plane at each period of the vibration, that the number of collisions goes to infinity in a finite time, and that the relative velocities decrease exponentially.

In the following, this collapsed phase is not investigated. Our study is restricted to values of γ smaller than 3. We only study the gas phase and the partially condensed phase where a cluster of particles appears at the bottom of the heap. Numerical simulations of this model have been performed with $h(t)$ chosen as a sawtooth function or a piecewise quadratic function for a wide range of parameters.

The model studied here is basically time dependent. However, all equations are time independent. In principle, all the distribution functions should always be periodic functions of time (with the period τ_0 of the plane). However, this dependency is irrelevant at small τ. For small τ, this model has the advantage of simplicity from both numerical and analytical points of view.

This publication is organized in the following manner. The relevant parameters of this model are presented in Sec. II. In Sec. III, the idea of pseudoparabola is introduced and used to estimate the constraints in numerical simulations. Section IV is devoted to the small damping regime (gas phase) and Sec. V to the strong damping regime where a cluster appears above $\gamma \sim 2.6$. Concluding remarks are presented in Sec. VI.

II. THE RELEVANT PARAMETERS

The first relevant parameter is γ rather than η and N. This fact already appears in previous papers [19,20]. This has been validated numerically for various N and η. Only a few numerical results are presented here. Figure 1 shows that the density profile $\rho(z)$ does not depend separately on N and η if N is large enough (say a few tens). We checked that this remains true for all γ between 0 and 3.

Indeed, if N is large enough (and τ is small), the one-body distribution function $P(z,v)$ [$\int P(z,v)dzdv = 1$] in the bulk is described by a Boltzmann equation which reads (see Appendix A and [21,22])

$$v\partial_z P - g\partial_v P = \frac{\gamma}{2}\int dv_1 P(z,v_1)\partial_v \times [|v-v_1|P(z,v)(v-v_1)]\,. \tag{5}$$

This equation depends on N only through the parameter γ. The boundary conditions are the following: $P(z,v)$ goes to zero as z or v goes to infinity and at $z = 0$, $P(z=0, v>0)$ (just after the bounce on the plane) is related to $P(z=0, v<0)$ (just before the bounce) by the velocity distribution of the plane. These conditions are independent of N. Thus, in this limit $P(z,v)$ should depend only on γ.

On the other hand, τ can be seen as a renormalized period of the plane. For all $\gamma < 3$, when τ is of the order of 1, the beads vibrate in phase with the plane. Small values of τ correspond to high frequencies for the plane: there is no phase locking between the plane and the heap and the motion of the plane can be considered as random. This property strongly simplifies the analytical approach and we restrict this study to small values of τ. Figure 2 shows that the density profile $\rho(z)$ is independent of τ, provided τ is small enough. All numerical results presented in the following are for small values of τ.

In previous experimental studies [14], the parameter $g\tau_0/V$ is considered instead of τ. If this parameter is less

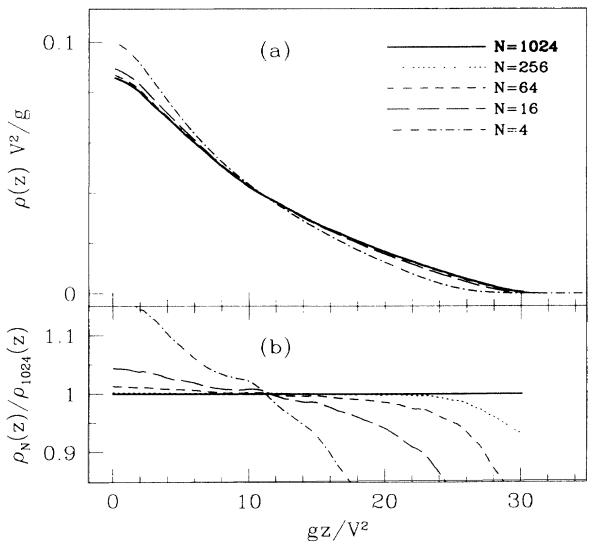

FIG. 1. Comparison of normalized density profiles $\rho_N(z)$ at $\gamma = 0.3$ and $\tau = 0.001$ for various values of N. (a) Density profiles, and (b) ratio $\rho_N(z)/\rho_{1024}(z)$.

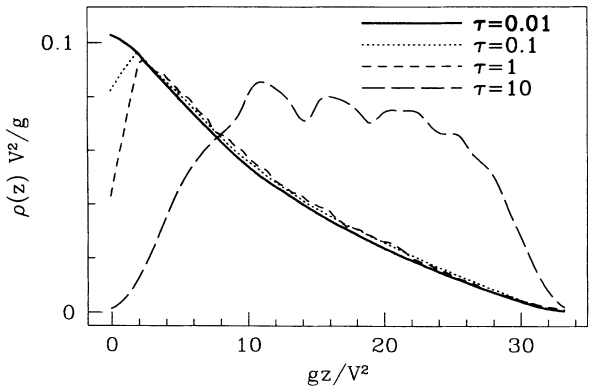

FIG. 2. Comparison of normalized density profiles $\rho(z)$ at $\gamma = 0.3$ and $N = 256$ for various values of τ.

than some constant (say $1/2\pi$), the acceleration of the plane becomes smaller than the gravity and the column sticks to the plane. This is correct for large enough γ. But, in the elastic limit ($\gamma = 0$), this solution becomes unstable. Therefore, the threshold of this sticking must depend on γ and the previous criterion is not correct. The choice of τ instead of $g\tau_0/V$ is justified in Sec. IV. The difference between these two parameters is important only for small γ. Indeed, for small γ, we never find that the column sticks to the plane.

III. REMARKS ON NUMERICAL SIMULATIONS

For simplicity, we choose a sawtooth function or a piecewise quadratic function of time for $h(t)$. For small values of N, the dynamics is not always ergodic. For example, at $\gamma = 0.01$ and $N \leq 5$, the trajectories exhibit fixed points in the velocity space when $h(t)$ is a sawtooth function; at larger γ, no fixed point has been observed. This problem is characteristic of the one-dimensional dynamics and in higher dimensions the dynamics is expected to be mixing. So, for our purpose, the shape of the plane function does not change the basic physics of the problem, as long as $\eta \neq 1$ and N is sufficiently large. Numerical simulations have also been done using a sinusoidal function $h(t)$ [19].

When $\eta = 1$, the velocities are exchanged during the collisions. Thus it is simpler to consider all trajectories as a set of parabolas. At $\eta = 1$, these parabolas are independent (this is only true in one dimension). For $\eta \neq 1$, the parabolas become "pseudoparabolas" (PPs) (see Fig. 3), because they have angular points at each collision corresponding to energy dissipation (see Fig. 3 at $\gamma = 3$). The collisions couple the PPs together and make the system mixing. These pseudoparabolas can be derived from the Boltzmann equation [Eq. (5)]. Indeed the right-hand side of Eq. (5) is just a derivative with respect to v. Thus the force acting on a particle is $-g - \frac{\gamma}{2}\int dv_1 P(z,v_1)|v - v_1|(v - v_1)$. $P(z,v)$ can be seen as a linear combination of pseudoparabolas

$$f(z,v) = \frac{1}{|v|}\delta(v - U(z)) \tag{6}$$

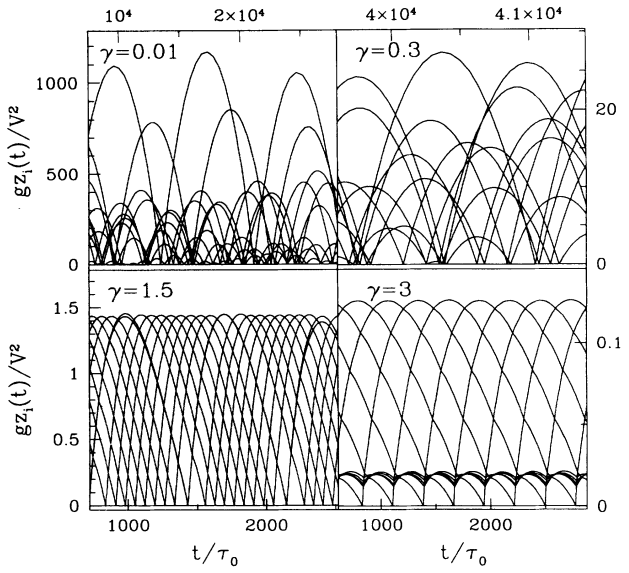

FIG. 3. Example of "pseudoparabolas" for systems of $N = 10$ beads and $\tau = 10^{-3}$ for various values of γ.

provided $U(z)$ satisfies

$$dU/dt = UdU/dz = -g - \frac{\gamma}{2}G(z,U), \tag{7}$$

where

$$G(z,U) = \int (U - v)P(z,v)|U - v|dv. \tag{8}$$

Except at a collision, a bead belongs to only one PP; thus the number of PPs is equal to the number of beads. In order to reach the steady state, it is important that each PP undergoes a large enough number n_0 of collisions with the plane. When the coupling between the PPs is weak ($\gamma \ll 1$), n_0 is estimated by considering the PPs to be independent. Let us call U_n, the velocity of a PP just after the nth collision with the plane. At each collision with the plane, the variation of U_n is of the order of V. As shown below, U_n follows a diffusion process in the velocity space and a typical velocity is of the order of $V/\sqrt{\gamma}$. Therefore, n_0 is of the order of the number of steps of a random walk in the velocity space going from 0 to $V/\sqrt{\gamma}$ by step $\sim V$. Thus n_0 scales as $1/\gamma$. At large γ, the coupling between the PPs is strong and the system reaches a steady state very rapidly; therefore, n_0 is chosen to be 1. In all cases, the total number of collisions with the plane scales as N/γ and the total number of collisions as N^2/γ, in order to reach a steady state.

The central function studied in this paper is the steady one-body distribution function $P(z,v)$. It is calculated by evaluating the exact amount of time spent by each particle in the range $[z, z + \Delta z]$ and $[v, v + \Delta v]$. We take a grid of 200 points in z and 200 points in v. A typical run consists of ten blocks of N/γ collisions with the plane ($\sim N^2/\gamma$ collisions in the bulk). In the first half of the runs, we check if equilibrium is reached: for each block, the energy provided by the plane, the maximum height of the column, the total number of collisions, and the time

spent per block are computed. In the second half of the runs, $P(z,v)$ is computed.

IV. THE LIMIT OF SMALL γ

The purpose of this section is to find the limit of $P(z,v)$ at small damping γ. But, as γ goes to 0, the energy and the height of the heap diverge. In this limit the trajectories obeying Eq. (7) should be close to parabolas. The natural approximation is to suppose, on the right-hand side of Eq. (8), that the particles follow exactly a free dynamics; thus we set $P(z,v)=P(0,(v^2+2gz)^{1/2})$ and $U^2(z)+2gz=U^2(0)$. Integrating Eq. (7), the resulting damping for a complete parabola starting at $z=0$ with velocity U is

$$\delta(U^2/2)=-\gamma\int_0^{U^2/2g}dzG(z,U(z)). \tag{9}$$

Thus a PP, starting with a velocity $U>0$ at $z=0$, later hits the plane with a velocity

$$-U(1-k(U))=-[\delta(U^2)+U^2]^{1/2}. \tag{10}$$

To first order in γ, Eq. (9) provides, after integration with respect to z,

$$k(U)=\frac{\gamma}{g}\Big\{2\int_0^U dvv^2P(0,v)+\frac{4}{3}U\int_U^\infty dvvP(0,v) -\frac{2}{3U^2}\int_0^U dvv^4P(0,v)\Big\}. \tag{11}$$

The next step is to tackle the interaction of the PP with the plane. In Appendix B, we show that the dynamics is equivalent to a diffusion process leading to an invariant probability distribution

$$P(0,U)=C\exp\left(-\frac{1}{2V^2}\int_0^U k(v)vdv\right) \tag{12}$$

for $U>0$. But, at first order in γ, $P(z,v)$ is a function of v^2+2gz and therefore

$$P(z,v)=C\exp\left(-\frac{1}{2V^2}\int_0^{\sqrt{v^2+2gz}}k(x)xdx\right) \tag{13}$$

with the normalization condition

$$\begin{aligned}1&=\int_0^\infty dz\int_{-\infty}^\infty dvP(z,v)\\&=\int_0^\infty dz\int_{-\infty}^\infty dvP(0,\sqrt{v^2-2gz})\\&=\frac{2}{g}\int_0^\infty dUP(0,U)U^2.\end{aligned} \tag{14}$$

Equations (11), (12), and (14) provide a closed set of equations for $P(0,U)$, $k(U)$, and C. In Appendix B, we solve this set of equations. Using the new dimensionless variables $\tilde{v}=U\sqrt{\gamma}/V$ and $\tilde{z}=zg\gamma/V^2$, we obtain a set of equations for $\tilde{k}(\tilde{v})=k(U\sqrt{\gamma}/V)/\gamma$ and the probability distribution $\tilde{P}(\tilde{z},\tilde{v})$ independent of γ. Thus the main consequence is that, as γ goes to 0, the typical velocity is $V/\sqrt{\gamma}$ and the typical height is $V^2/g\gamma$.

The computed velocity distribution $P(0,U)$ and density profile $\rho(z)$ are shown in Figs. 4(a) and 4(b). These distributions agree with the theoretical results. $P(0,U)$ becomes symmetric as γ goes to 0. At large $\tilde{v}$, the velocity distribution is roughly Gaussian as in a perfect gas and the density distribution decreases exponentially.

The convergence to the theoretical curves is fast as γ goes to 0. As γ increases, the dissymmetry of $P(0,U)$ increases [see Fig. 4(a)]. In Fig. 5, we compare the function $k(U)$ obtained from this theory and by differentiation of the numerical $P(0,U)$. Such a differentiation of numerical results magnifies statistical fluctuations. Nevertheless, reasonable agreement is found at $\gamma=0.01$. But, at larger γ, $k(U)$ increases with U well above 1, which implies that $P(0,U)$ vanishes more rapidly than a Gaussian function. For the sake of clearness, the asymptotic behaviors at small and large velocities are not reported in Fig. 5, but Eqs. (B3) and (B4) of Appendix B are a good approximation up to $\tilde{v}=3$ and 3.5, respectively.

It is important to determine the values of τ for which the model is valid. This model is based on the hypothesis that the duration of a pseudoparabola is much larger than the period τ_0 of the vibration. For a particle having an initial velocity $\sim V/\sqrt{\gamma}$, the condition reads $\tau\ll 1$, where τ is defined in Eq. (4). In the (γ,τ) plane, the validity domain of this model is around the origin. In this domain, the results do not depend on the shape of the vibration of the plane. Indeed, from numerical simulations with a piecewise parabolic shape, we found the same results within statistical uncertainties.

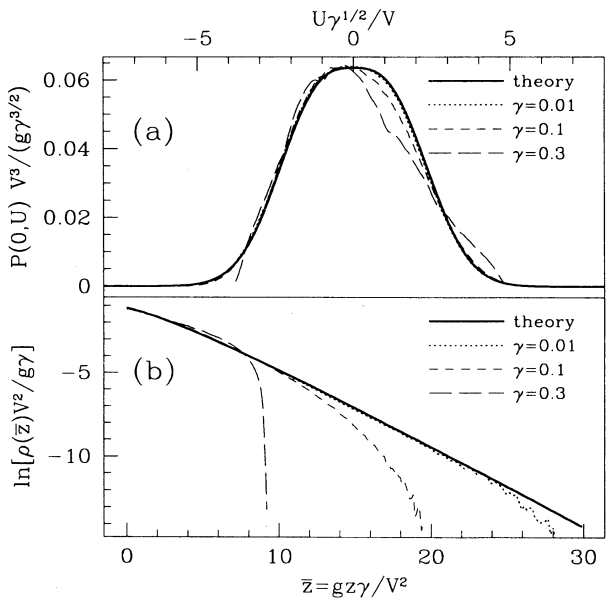

FIG. 4. Comparison of the velocity distributions obtained by numerical simulations and by the theory at small γ. (a) Velocity distribution at the bottom of the column $P(0,U)$; and (b) density profile $\rho(z)$.

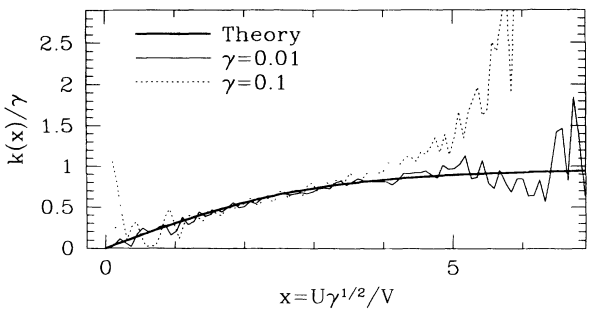

FIG. 5. Comparison of the function $k(x)$ obtained by numerical simulations at small γ with the solution of the set of equations (B2).

V. THE STRONG DAMPING REGIME ($1.5 < \gamma < 3$)

In the previous case ($\gamma \ll 1$), we used a symmetric distribution of velocities at each abscissa maximum at $v = 0$. When γ increases, this distribution becomes more and more asymmetric. The upward particles have a velocity significantly larger than that of the downward particles. Fortunately, a solution of the Boltzmann equation for large γ can be found, which works in the case of a sawtooth vibration of the plane. This is achieved with a self-consistent solution of Eqs. (7) and (8), where $P(z,v)$ in Eq. (8) is the density corresponding to the PP solution of Eq. (7). Thus all PPs have the same trajectory (see Fig. 3). Let $v_+(z) > 0$ [$v_-(z) < 0$] be the velocity of the upward (downward) particles. Thus $P(z,v)$ can be chosen as

$$P(z,v) = (Cg/V)\{[1/v_+(z)]\delta(v - v_+(z)) - [1/v_-(z)]\delta(v - v_-(z))\}, \quad (15)$$

where C is a dimensionless constant and Eq. (8) reads

$$G(z, v_\pm) = -\frac{Cg}{V}\frac{(v_+ - v_-)^2}{v_\mp}. \quad (16)$$

In Appendix C, we find a solution of Eqs. (7) and (16), provided $1.5 < \gamma < 3$. From $\gamma = 1.5$ to $\gamma \simeq 2.5$, we found good agreement with the simulations (the case of the sawtooth vibration) (see Fig. 6).

Above $\gamma \approx 2.5$, simulations present a sharp peak in $\rho(z)$, close to the plane and growing with γ. This peak corresponds to the appearance of a cluster of beads almost at rest and in levitation near the bottom of the heap. More precisely, this system may be seen as an ensemble of PPs and a bunch of new trajectories almost at rest which never reach the plane. The cohesion of this cluster is ensured by its inelastic collisions with the PPs. This is what we call the partially condensed phase. In Appendix C, we show that another analytical solution appears at $\gamma = \sqrt{6} \simeq 2.45$. This solution will be used for comparison with numerical simulations for $\gamma > \sqrt{6}$.

Figure 6(a) shows the density profile for different values of γ. The dashed curves hold for the predicted densities [Eq. (C3) of Appendix C]. Good agreement with the

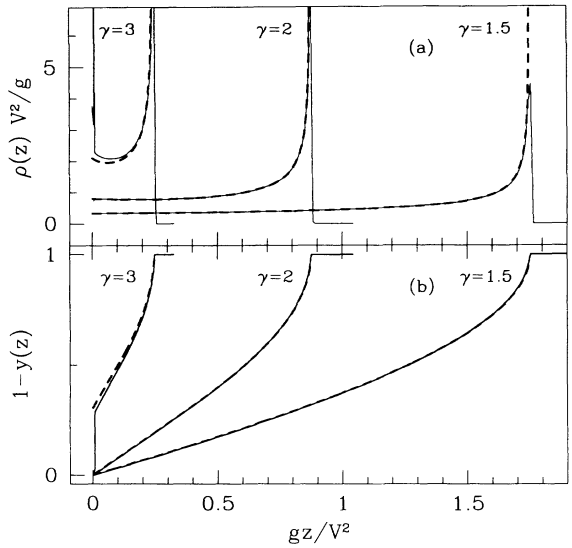

FIG. 6. Density profiles at $\gamma \geq 1.5$. Full line, numerical simulations results; dash lines, theoretical curves. (a) Density profiles [Eq. (C3)] and (b) integrated density profile presenting a step at $z = 0$ for $\gamma > \sqrt{6}$.

predicted location of the top of the stack was found. The singularity in $1/\sqrt{z_{\max} - z}$ for the density near the top is the direct consequence that the velocity distribution is a well defined Dirac function. Figure 6(b) shows the integrated density profile. For $\gamma > \sqrt{6}$, the theoretical curve has a jump at $z = 0$ corresponding to the peak supposed to be at the bottom, while in the simulation the peak is at a small altitude z_0 (larger than the amplitude of the vibration). But they both give approximately the same height for the jump.

For γ close to 1.5, the velocity distribution consists of two very sharp peaks. As γ increases the peaks slowly stretch. For $\gamma > \sqrt{6}$, near the bottom, the negative peak becomes a rough heap around zero.

Before we used a sawtooth vibration. It is important to look at a more general vibration in order to check whether the transition to a partially condensed phase is relevant. For a piecewise quadratic vibration, the analytical calculations are much more difficult. On the plane, an incident particle of small velocity v will produce an output velocity in the range $[v^2/V, \sqrt{vV}]$. Thus we should be far from the result of the sawtooth vibration. In particular, the velocity distribution is no longer a Dirac function and therefore the singularity of $\rho(z)$, at the top of the heap, does not exist anymore.

In Fig. 7(a), we compare the integrated density for the sawtooth and the piecewise quadratic models. For the sawtooth vibration the maximum of the density is at the top, while for the piecewise quadratic vibration the density is decreasing. The maximum values for z are of the same order of magnitude, but are different.

For fixed γ the mean square velocity V should be rescaled in order to compare these models. Indeed, as γ increases, the velocity of the incident beads decreases. Thus the collisions with the plane occur when the plane is near its maximum. Consequently, the plane velocity

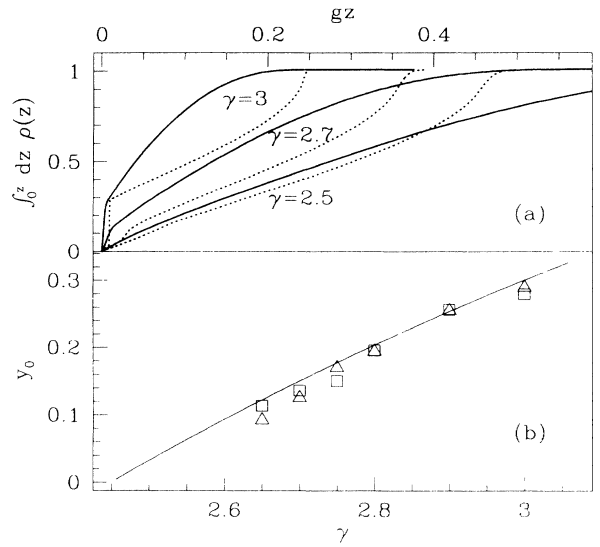

FIG. 7. Comparison of partially condensed phase in the two models. (a) Integrated density profile: full lines, sawtooth vibration; dotted lines, piecewise quadratic vibration. (b) Ratio of the clustered beads just above the plane: full line, analytical solution of the sawtooth vibration model [Eqs. (C6)]; triangles, numerical simulation estimations with a sawtooth vibration; squares, numerical simulation estimations with a piecewise quadratic vibration.

during a collision diminishes as γ increases. On the other hand, for the sawtooth vibration, the plane velocity is always V.

Although the density functions may differ, we see, in Fig. 7(b), that the size of the cluster, at the bottom of the heap, y_0 is the same in these two models and in agreement with theoretical values (for $\gamma < 2.6$, the cluster is loosely packed and it is practically difficult to estimate its size). Thus the partially condensed phase seems well defined by γ, which is the only dimensionless parameter.

VI. CONCLUSION

Our simulations have been carried out with a sawtooth and a piecewise quadratic function $h(t)$.

For small γ ($\gamma < 0.1$), the results do not depend on $h(t)$. This has been shown analytically [for any choice of square integrable $h(t)$] and numerically.

For large γ ($\gamma > \gamma_c$) the heap collapses on the plane (at least during a fraction of the period of the plane). The precise determination of the critical γ_c will be subject of another paper.

For intermediate γ ($1.5 < \gamma < 3$), the mean square velocity V must be slightly corrected [only the top part of $h(t)$ is accessible to the collisions] and the density distributions may vary with the shape of $h(t)$, but the important result is that the transition between the gas and the partially condensed phases does not depend on $h(t)$ and is only defined by γ. As γ increases, the velocity of the incident beads decreases; thus only the top part of the function $h(t)$ becomes relevant. The piecewise quadratic function $h(t)$ becomes a general model for any twice differentiable function $h(t)$ (with nonzero and finite curvature at the maximum), while the sawtooth function $h(t)$ is still a different model. It is therefore important that these models provide the same thresholds and the same ratio of clustered beads.

The partially condensed phase can be explained as follows. The dissymmetry of the velocity distribution in the bulk increases as γ increases or z decreases. Thus the acceleration for a test bead at rest ($U \simeq 0$), given by Eq. (7), is maximum at $z = 0$ and increases as γ increases. At $\gamma = \sqrt{6}$, the sawtooth model shows that the term $G(0,0)$ compensates for the gravity. The acceleration at the bottom of the heap is just 0. For larger γ, the acceleration at the bottom should be positive. Thus a new kind of trajectory can occur: trajectories which never reach the plane. In fact, the system chooses to pack a cluster of beads at rest at the bottom of the heap ensuring that the maximum acceleration is always 0 at the bottom. This mechanism is not specific to one-dimensional models and we expect the same kind of transition for more realistic models in two or three dimensions.

ACKNOWLEDGMENTS

The Laboratoire de Physique Théorique des Liquides is Unité de Recherche Associée au Centre National de la Recherche Scientifique No. 765. The Centre de Physique Théorique is Unité de Recherche Propre du Centre National de la Recherche Scientifique No. 14.

APPENDIX A

The stationary Boltzmann equation for the one-body distribution function $P(z,v)$ [$\int P(z,v)dzdv = 1$] reads

$$v\partial_z P - g\partial_v P = F(P), \tag{A1}$$

where $F(P)$ describes the collisions between particles. In fact, F should depend on the correlation function $P_2(z,v_1,v_2)$, but at first order $P_2(z,v_1,v_2) \simeq P(z,v_1)P(z,v_2)$. For completeness, we quickly derive this equation, which has already been established in [22]. Let us calculate the collision term $F(P)$. At given z and v, the variation of the number of particles $NP(z,v)dzdv$ per unit of time due to collisions is estimated. The first term corresponds to the decrease of the density as a particle of velocity v hits another one:

$$N^2 P(z,v)dzdvP(z,v_1)|v - v_1|dv_1. \tag{A2}$$

The second collision term corresponds to the increase of the density as a particle of velocity v_2 hits another particle and the resulting particle velocity falls into the interval $[v, v + dv]$. For each unit of time, this collision term gives

$$N^2 P(z,v_2)dzdv_2 P(z,v_1)|v_2 - v_1|dv_1 \tag{A3}$$

with $v = v_2 - (1-\eta)(v_2 - v_1)/2$ and $dv_2(1+\eta)/2 = dv$.

The difference of these terms [Eq. (A3) minus Eq. (A2)] provides

$$N^2 dz dv P(z,v_1)\Big[\frac{2}{1+\eta}|v_2-v_1|P(z,v_2) - |v-v_1|P(z,v)\Big]dv_1.$$

In the limit of small $1-\eta$ (large number of particles), we get, to first order,

$$\begin{aligned}\frac{2}{1+\eta}|v_2-v_1|P(z,v_2) - |v-v_1|P(z,v) &\simeq \frac{1-\eta}{2}\{(v-v_1)\partial_v[|v-v_1|P(z,v)] \\ &\quad +|v-v_1|P(z,v)\} \\ &= \frac{\gamma}{2N}\partial_v[|v-v_1|P(z,v)(v-v_1)],\end{aligned}$$

leading to the Boltzmann equation (5) after integrating the collision term with respect to v_1.

APPENDIX B

In this appendix, we provide the solution of $P(z,v)$ at small damping γ. Let us first solve the boundary condition at the bottom of the plane. For fixed V [Eq. (2)] and τ_0, as γ goes to zero, the bead velocities increase to infinity and the time between two bounces diverges. In this limit, our model becomes equivalent to a random model where the collisions with the plane occur at $z=0$ and the plane velocity V_p at each bounce may be chosen at random with the law $r(V_p)dV_p$, the probability distribution of $V_p(t)$.

Let U_n be the velocity of a PP just after the nth collision with the plane. Just before the $(n+1)$th collision with the plane, this velocity is $-U_n(1-k(U_n))$, according to Eq. (10). Thus, after the $(n+1)$th collision, we have

$$U_{n+1} = [1-k(U_n)]U_n + 2V_p. \tag{B1}$$

It is important to notice that the probability to find a velocity V_p, at the $(n+1)$th collision, is proportional to the relative velocity (V_p+U_n) and to $r(V_p)dV_p$ (we assume $|U_n| \gg |V_p|$ so that V_p+U_n is positive). So, such an iteration occurs with probability $(1+V_p/U_n)r(V_p)dV_p$. Thus the conditional expectations of U_{n+1} and U_{n+1}^2 are

$$\begin{aligned}E(U_{n+1}|U_n) &= \int dV_p r(V_p)\{[1-k(U_n)]U_n + 2V_p\} \\ &\quad \times(1+V_p/U_n) \\ &\simeq [1-k(U_n)]U_n + 2V^2/U_n,\end{aligned}$$

$$\begin{aligned}E(U_{n+1}^2|U_n) &= \int dV_p r(V_p)\{[1-k(U_n)]U_n + 2V_p\}^2 \\ &\quad \times(1+V_p/U_n) \\ &\simeq [1-k(U_n)]^2U_n^2 + 8V^2.\end{aligned}$$

The sequence of U_n can be approximated by a continuous diffusion process with drift

$$F = E(U_{n+1}|U_n) - U_n \simeq -k(U_n)U_n + 2V^2/U_n$$

and variance

$$\sigma^2 = E(U_{n+1}^2|U_n) - E(U_{n+1}|U_n)^2 \simeq 4V^2.$$

The invariant probability distribution $f(U)$, associated with this drifted diffusion process, is the solution of

$$\frac{1}{2}\partial_U[\sigma^2 f] - Ff = 0.$$

One obtains $f(U) = C'U\exp[-\int_0^U k(v)vdv/2V^2]$. $f(U)$ is the flow of the particle through $z=0$, that is, $f(U)$ is proportional to $UP(0,U)$, and thus we get Eq. (12).

Let us now give the final solution for $P(z,v)$. Equations (11), (12), and (14) provide a closed set of equations for $P(0,U)$, $k(U)$, and C. Using the scaling $\tilde{k}(x) = k(xV/\sqrt{\gamma})/\gamma$, $\tilde{P}(x) = P(0,xV/\sqrt{\gamma})V^3/(g\gamma^{3/2})$, and $\tilde{C} = \tilde{P}(0) = CV^3/(g\gamma^{3/2})$, one expresses the previous equations as a dimensionless set of equations independent of γ:

$$\begin{aligned}\tilde{P}(x) &= \tilde{C}\exp\left(-\frac{1}{2}\int_0^x \tilde{k}(y)ydy\right), \\ 1 &= 2\int_0^\infty dx x^2\tilde{P}(x), \\ \tilde{k}(x) &= 2\int_0^x dy y^2\tilde{P}(y) + \frac{4}{3}x\int_x^\infty dy y\tilde{P}(y) \\ &\quad -\frac{2}{3x^2}\int_0^x dy y^4\tilde{P}(y).\end{aligned} \tag{B2}$$

Asymptotic behaviors of $\tilde{k}(x)$ are found in the two limits of small and large x. For small x, we find

$$\tilde{k}(x) = \frac{2\tilde{M}_1}{3}x - \frac{2\tilde{C}}{15}x^3 + \frac{\tilde{C}\tilde{M}_1}{540}x^6 + O(x^7), \tag{B3}$$

where

$$\tilde{M}_n = \int_{-\infty}^\infty dx\tilde{P}(x)|x|^n$$

are the moments of $\tilde{P}$. For large x, we find

$$\tilde{k}(x) = 1 - \frac{1}{x^2}\frac{\tilde{M}_4}{3} + O[\exp(-x^2/4)x^{\tilde{M}_4/6-3}]. \tag{B4}$$

Equation (B3) provides the shape of $\tilde{P}(x)$ at small x: $\tilde{P}(x) = \tilde{C}_1\exp(-\tilde{M}_1|x|^3/9)$. From Eq. (B4), we obtain at large x, $\tilde{P}(x) = \tilde{C}_2 x^{\tilde{M}_4/6}\exp(-x^2/4)$.

The system of Eqs. (B2) can be solved numerically by iterations. Starting from the simplest form $\tilde{k}(x) = \tilde{M}_1 x/3$ for $x < x_l = 3/\tilde{M}_1$ and $\tilde{k}(x) = 1$ for $x > x_l$, $\tilde{P}(x)$ is computed, then the normalization condition is applied, and a new function $\tilde{k}(x)$ is obtained. This method converges within few iterations giving $\tilde{C} = \tilde{P}(0) = 0.063\,554\,16$, $\tilde{M}_1 = 0.473\,087\,84$, $\tilde{M}_2 = 1$ [see Eq. (14)], and $\tilde{M}_4 = 8.035\,233\,93$. $\tilde{k}(x)$ is presented in Fig. 5 and $\tilde{P}$ in Fig. 4(a).

APPENDIX C

In this appendix, we calculate the density profile and the velocities of the PPs, in the case of a sawtooth vibration, by solving Eqs. (7) and (16). Instead of z, we use the variable $y(z)$ (omitting the z dependency of v_+, v_-, and y): $y = (Cg/V)\int_z^\infty [1/v_+(z') - 1/v_-(z')]\,dz'$. $y(z)$ represents the fraction of particles above the abscissa z. Thus, after integration of Eq. (7) we have

$$\begin{aligned} v_+ - v_- &= Vy/C, \\ v_+ + v_- &= \gamma V y^2/3C + VC_1/y, \\ \partial_z y &= -(Cg/V)(1/v_+ - 1/v_-), \end{aligned} \tag{C1}$$

where C and C_1 are dimensionless constants to be determined. At the top of the column, the boundary condition reads $y = 0$, and $v_+ = v_- = 0$, which yields $C_1 = 0$. Therefore, the solution for y is

$$y = \frac{3}{\gamma}\sqrt{1-\sqrt{1-\tilde{z}}}, \quad \tilde{z} = \frac{g}{V^2}\left(\frac{4C\gamma}{3}\right)^2 (z_{\max} - z). \tag{C2}$$

In contrast with the case of small γ, no particle can be found above $z_{\max}$, where y vanishes. The density profile is given by

$$\rho(z) = -\partial_z y = \frac{g}{V^2}\frac{4C^2\gamma}{3}\left(\frac{1+\sqrt{(1-\tilde{z})}}{\tilde{z}(1-\tilde{z})}\right)^{1/2}. \tag{C3}$$

The two parameters C and $z_{\max}$ are fixed by the boundary condition at $z = 0$. There we have $y = 1$ and $v_+ = 2V - v_-$ if we assume that the collisions with the plane occur only when the plane moves upward. This hypothesis reads $0 < -v_-(0) < V$. Thus we obtain $C = \gamma/6$ and

$$z_{\max} = \frac{V^2}{g}\left(\frac{9}{2\gamma^2} - 1/4\right). \tag{C4}$$

The conditions $0 < -v_-(0) < V$ provide now the domain of validity $1.5 < \gamma < 3$.

Now let us show that for $\gamma \approx 2.5$, another solution appears, which is in fact the stable solution. This solution corresponds to a cluster of N_0 particles at an altitude z_0. To model this phenomenon, we replace this cluster by a δ function in the distribution $\rho(z)$ and therefore $y(z)$ has, at z_0, a step of $y_0 = N_0/N$. Above z_0, the previous set of equations [Eqs. (C2)] remains true, where C and $z_{\max}$ are fixed by new boundary conditions. Assuming that the cluster is at rest at z_0, the velocities v_+ and v_-, above (z_0^+) and below (z_0^-) the cluster, are related by

$$v_+(z_0^+)/v_+(z_0^-) \approx \left(\frac{1+\eta}{2}\right)^{N_0} \approx e^{-\alpha} \approx v_-(z_0^-)/v_-(z_0^+), \tag{C5}$$

where $\alpha = \gamma y_0/2$ and Eq. (1) is used to treat the successive collisions with the N_0 beads at rest. Assuming also that only a few particles are under the peak in $\rho(z)$, the boundary conditions at the bottom now read $v_+(z_0^-) = -v_-(z_0^-) + 2V$ and $v_+(z_0^-) - v_-(z_0^-) = V/C$, that is,

$$\begin{aligned} v_+(z_0^+) &= Ve^{-\alpha}[1 + 1/(2C)], \\ v_-(z_0^+) &= Ve^{\alpha}[1 - 1/(2C)]. \end{aligned}$$

Substituting these expressions into Eqs. (C1) with $y = 1 - y_0$ leads to

$$\begin{aligned} (1-y_0)[\sinh(\alpha) + \gamma(1-y_0)/3\cosh(\alpha)] &= 2C, \\ (1-y_0)[\cosh(\alpha) + \gamma(1-y_0)/3\sinh(\alpha)] &= 1. \end{aligned} \tag{C6}$$

If $y_0 = 0$, we recover the previous solution. Another nonzero solution for y_0 appears at $\gamma = \sqrt{6} \simeq 2.45$. This new solution has been used for comparison with numerical simulations for $\gamma > \sqrt{6}$. Figure 7 shows the comparison of the solution y_0 of Eqs. (C6) and y_0 obtained by numerical simulations for both vibrations.

[1] P. Bak, C. Tang, and K. Wiesenfeld, Phys. Rev. Lett. **59**, 381 (1987).

[2] P. Evesque and J. Rajchenbach, Phys. Rev. Lett. **62**, 44 (1989).

[3] L. P. Kadanoff, S. R. Nagel, L. Wu, and S. M. Zhou, Phys. Rev. A **39**, 6524 (1989).

[4] A. Rosato, R. Strandbourg, F. Prinz, and R. H. Swendsen, Phys. Rev. Lett. **58**, 1038 (1987); R. Jullien, P. Meakin, and A. Pavlovitch, *ibid.* **69**, 640 (1992).

[5] J. Rajchenbach and P. Evesque, C. R. Acad. Sci. Paris Ser. II **307**, 1 (1988); P. Evesque and J. Rajchenbach, *ibid.* **307**, 223 (1988); S. B. Savage, J. Fluid Mech. **194**, 457 (1988); S. Fauve, S. Douady, and C. Laroche, J. Phys. (Paris) Colloq. **50**, C3-187 (1989); C. Laroche, S. Douady, and S. Fauve, J. Phys. Paris **50**, 699 (1989); S. Douady, S. Fauve, and C. Laroche, Europhys. Lett. **8**, 621 (1989).

[6] O. Zik and J. Stavans, Europhys. Lett. **16**, 255 (1991); O. Zik, J. Stavans, and Y. Rabin, *ibid.* **17**, 315 (1992); Y. H. Taguchi, Phys. Rev. Lett. **69**, 1367 (1992); J. A. C. Gallas, H. J. Herrmann, and S. Sokolowski, *ibid.* **69**, 1371 (1992).

[7] P. K. Haff, J. Fluid Mech. **134**, 401 (1983).

[8] P. Evesque, E. Szmatula, and J. P. Denis, Europhys. Lett. **12**, 623 (1990).

[9] R. A. Bagnold, Proc. R. Soc. London Ser. A **225**, 49 (1954).

[10] S. B. Savage, J. Fluid Mech. **92**, 53 (1979).

[11] J. T. Jenkins and S. B. Savage, J. Fluid Mech. **130**, 187 (1983); J. T. Jenkins and M. W. Richman, Phys. Fluids **28**, 3485 (1985).

[12] H. Caram and D. C. Hong, Phys. Rev. Lett. **67**, 828

(1991).
[13] M. Y. Louge, J. T. Jenkins, and M. A. Hopkins, Phys. Fluids A **2**, 1042 (1990); G. C. Barker and A. Mehta, Phys. Rev. A **45**, 3435 (1992).
[14] E. Clément and J. Rajchenbach, Europhys. Lett. **16**, 133 (1991); E. Clément, J. Duran, and J. Rajchenbach, Phys. Rev. Lett. **69**, 1189 (1992).
[15] M. A. Hopkins and M. Y. Louge, Phys. Fluids A **3**, 47 (1991).
[16] S. McNamara and W. R. Young, Phys. Fluids A **4**, 496 (1992).
[17] A. Mehta and J. M. Luck, Phys. Rev. Lett. **65**, 393 (1990).
[18] B. Bernu and R. Mazighi, J. Phys. A **23**, 5745 (1990).
[19] E. Clément, S. Luding, A. Blumen, J. Rajchenbach, and J. Duran, J. Mod. Phys. B **7**, 1807 (1993).
[20] S. Luding, E. Clément, A. Blumen, J. Rajchenbach, and J. Duran, Phys. Rev. E **49**, 1634 (1994).
[21] G. F. Carnevale, Y. Pomeau, and W. R. Young, Phys. Rev. Lett. **64**, 2913 (1990).
[22] S. McNamara and W. R. Young, Phys. Fluids A **5**, 34 (1993).